

# Biogenic particles in the surface microlayer and overlaying atmosphere in the central Arctic Ocean during summer

By CAROLINE LECK<sup>1\*</sup> and E. KEITH BIGG<sup>2†</sup>, <sup>1</sup>*Department of Meteorology, Stockholm University, S-10691 Stockholm, Sweden;* <sup>2</sup>*The International Meteorological Institute in Stockholm, S-10691 Stockholm, Sweden*

(Manuscript received 17 September 2004; in final form 24 January 2005)

## ABSTRACT

Transmission electron microscopy photographs of airborne particles are compared with those of particles found in the surface microlayer of the open water between ice floes in the central Arctic Ocean in summer. The similarity in morphology, physical properties, X-ray spectra and a chemical reaction of the numerous aggregates and their building blocks predominantly smaller than 70 nm diameter, and of bacteria and other micro-organisms found in both, strongly suggests that the airborne particles were ejected from the water by bursting bubbles. The shape of the size distribution of aggregates in the air is very similar to that in the water, each with a well-defined Aitken mode but shifted towards smaller sizes. Diffuse electron-transparent material joining and surrounding the heat resistant and non-hygroscopic particulates in both the air and water is shown to have properties consistent with the exopolymer secretions (EPS) of microalgae and bacteria in the water. EPS are highly surface-active, highly hydrated molecules that can spontaneously assemble into gels. They are broken down by ultraviolet light or acidification. These properties provide an explanation for the different resistance to dehydration of bacteria from air and water samples when subjected to a vacuum, and the apparent absence of sea salt on airborne bacteria and aggregates. The difference in size distribution between the air and water samples is also explained. The role of EPS and particulate matter from the open lead surface microlayer in the production of the airborne Aitken mode particles and cloud condensation nuclei is examined and concluded to be very important.

## 1. Introduction

Leck and Bigg (1999) and Bigg and Leck (2001) described the occurrence of non-hygroscopic crystalline and quasi-crystalline airborne particles often with pentagonal or hexagon habits in sizes of 10–50 nm diameter found over the Arctic Ocean pack ice in summer during the Arctic Ocean Expedition of 1996 (AOE-96, Leck et al., 2001). High concentrations were associated with increased concentrations of liquid organic particles having volumes equal to those of ~100 nm spheres. They were also associated with enhanced concentrations of larger (~100–300 nm diameter spheres) particles clearly of marine origin, such as bacteria and fragments of diatoms. It was proposed that particles of the last two types were ejected by bursting bubbles into the air from the open water surfaces (“open leads”) between ice floes (Leck et al., 2002). At that time, however, there was no evidence concerning the origin of the airborne non-hygroscopic particulates, but in both shape and size they resembled the “mi-

crocolloids” described by Wells and Goldberg (1991) and others in lower-latitude oceanic water.

In a subsequent Arctic Ocean expedition (AOE-2001) in 2001, Knulst et al. (2003) collected samples of water from the surface microlayer of the open leads (SMOL) using radio-controlled boats. Samples of this water were examined for insoluble particulates by Bigg et al. (2004). They found concentrations ranging from  $2 \times 10^7$  to  $>10^{14}$  ml<sup>-1</sup>. Size distributions of the particles (photographed with a transmission electron microscope (TEM)) were also very variable, with modal diameter sizes of 10 nm in some samples and 40 nm in others, the 40 nm particles appearing to be aggregates of the 10 nm ones. A diffuse almost electron-transparent material held the particles together in rafts, strings or balls. Bigg et al. (2004) considered that the diffuse fluid material could be related to the “mucus-like” material bridging microcolloids described by Wells and Goldberg (1991). Moreover, bacteria were found, sometimes in groups joined by nearly electron-transparent material. They were typically from 600 to 3000 nm in length and having widths one-third of their length. Epifluorescence microscopy showed their concentrations to vary within the range  $1.2 \times 10^6$  to  $1.8 \times 10^6$  ml<sup>-1</sup>, far less than the orders of magnitude variation of the particulate concentrations.

\*Corresponding author.  
e-mail: lina@misu.su.se

†Present address: 12 Wills Ave., Castle Hill 2154, Australia.

Some much smaller particles near the bacteria resembled bacteriophage viruses. Fragments of diatoms and other suspected micro-organisms were also present.

This paper will describe the high Arctic airborne, apparently non-hygroscopic, particulates, bacteria and micro-organisms collected during AOE-2001 that were very similar to those found during AOE-96. They will then be compared with simultaneously collected SMOL particulate matter in order to see which, if any, of the airborne particles might have been ejected into the atmosphere by bursting bubbles on the water surface. The reason for doing so is that the concentration of cloud condensation nuclei (CCN) influences cloud properties, precipitation processes and possibly climate. While the water-insoluble particles of the SMOL would be inactive as CCN, they could in principle act as nuclei for the condensation of oxidation products of dimethyl sulfide (DMS), a gas released in the uppermost ocean surface from dying phytoplankton (Leck et al., 1990; Leck and Persson, 1996). The diffuse, electron-transparent and apparently fluid material in the SMOL is likely to accompany particles that enter the air as a result of bursting of bubbles on the water surface. If present it may have significance for cloud formation, so its detection and a study of its properties are further aims of this work.

## 2. Time and location

Airborne particle collections were made from on-board the Swedish icebreaker *Oden* during an expedition to the central Arctic Ocean from 5 July (day of year (DOY) 186) to 26 August (DOY 238) 2001 (Leck et al., 2004) whenever there was no possibility of contamination from shipboard sources. Most of the results were obtained during the period 2 (DOY 214) to 21 (DOY 233) August when the ship was moored to, and drifted with, an ice floe from latitude 88.9°N to 88.2°N. The rectangle of Fig. 1 marks the area in which samples were collected. The figure also shows the southern limit of the central Arctic Ocean ice, having a 20–70% cover in the marginal ice zone to 80–95% in the pack ice zone. In the latter, ice floes were up to several kilometres in diameter, with thicknesses ranging from 1.5 to 8 m about an average of 2.5 m. Between them were irregular open water channels—the open leads—from a few metres up to an occasional 2000 m in width. The surface mixed layer of the ocean was only 20–30 m deep, had a salinity of about 32 psu (practical salinity units) and an almost constant temperature near  $-1.7^{\circ}\text{C}$ . Surface air temperatures were usually in the range  $-1.5$ – $0^{\circ}\text{C}$  and the sun was continuously above the horizon at all stations, though commonly obscured by cloud.

## 3. Methods

### 3.1. Airborne particle collection

Leck et al. (2001) have described in detail the location of the air inlets and instruments on-board the icebreaker *Oden*. The air

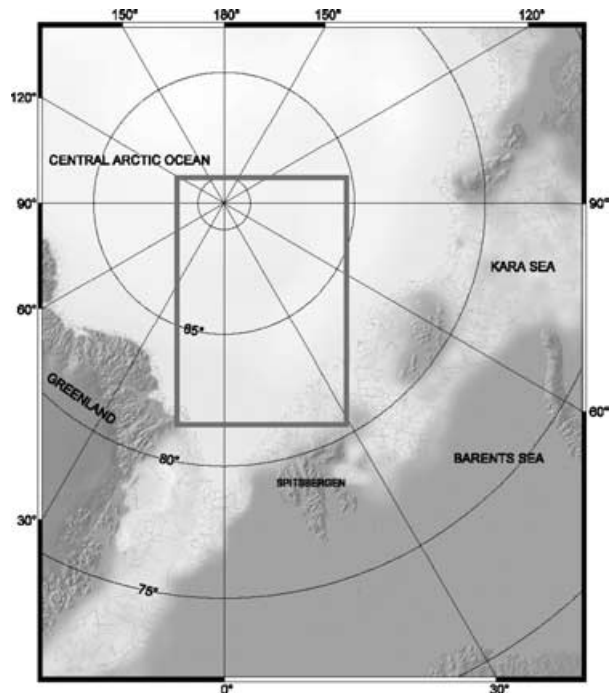


Fig. 1. Map showing the route of AOE-01, and the area in which concentrated studies of airborne particles and the SMOL were made while drifting with the ice. Also shown is the region covered by pack ice.

for subsequent collection was drawn in via a sampling manifold located at 27 m above sea level. An Anderson impactor having a  $10\ \mu\text{m}$  diameter cut size for particles was located at the inlet of the manifold. A pollution sensor prohibited direct contamination from the ship. Particles were collected directly onto 3 mm copper TEM grids having a polyvinylbutyral (“butvar”) collecting surface. There were three collectors:

(1) An impactor having a 500 nm diameter round tapered nozzle, a flow rate of  $30\ \text{ml s}^{-1}$  and a theoretical collection efficiency of 50% for particles having an effective aerodynamic diameter (EAD) of 160 nm and a relative density 1.5, or 200 nm EAD particles with a relative density of 1.

(2) A low-flow ( $1.3\ \text{ml s}^{-1}$ ), low-pressure impactor using a  $75\ \mu\text{m}$  circular electron microscope aperture as its nozzle. Because the actual pressure at the collecting surface was not known its collection efficiency was not calculated, but some individual particles down to 20 nm were collected.

(3) An electrostatic precipitator. Particle charges were imparted at the air inlet by a  $^{63}\text{Ni}$   $\beta$ -emitting radioactive source and the particles precipitated by a  $12\ \text{kV cm}^{-1}$  electric field between air inlet and collecting surface. The flow rate was kept very low ( $0.17\ \text{ml s}^{-1}$ ) so that particles up to about  $1\ \mu\text{m}$  diameter could be collected. Collection efficiency depends on the unknown charging efficiency but probably fell off below 10–15 nm diameter.

### 3.2. Identification of the particles by morphology and chemical properties

To allow a 3-D structure to be deduced, and the diameter of a sphere of equivalent volume (DES) to be calculated, artificial shadows were imposed by vacuum evaporation of a metal onto the plastic collecting surface of the TEM grid, such that shadow length was twice the height of the particle. Platinum, silver or a chromium–nickel alloy were used. The metal coating also preserved the original outline of a particle that evaporated in an electron beam or otherwise changed during treatment. Obtaining high-quality photos from a TEM is a time-consuming process. With a huge number of specimens to be examined and a limited time available on a rented TEM (Philips CM-12, Sydney University Electron Microscope Unit), a compromise between quantity and quality was necessary in order to acquire an objective sample of the particles on a grid. The focus was set and an external hand-held digital camera was used to photograph every particle encountered in one or more scans across a grid, so that a representative and objective sample of the particles in the size range collected could be obtained. A few quality photographs of selected individual particles were then added to the collection.

After a first examination for morphology, the TEM grids were subsequently tested for various properties. Hygroscopicity was assessed by spreading of the particle when subjected to a high relative humidity, regulated by a glycerol–water solution. Solubility in various organic vapours was tested by the spreading of the particle when subjected to an atmosphere saturated with the vapour. Decane, xylene and cyclohexane were used. The failure of particles to dissolve in these vapours did not necessarily mean that the particles were not organic—polysaccharides and proteins for example would not react with those solvents. Heat resistance was assessed by the extent to which a particle evaporated when subjected to a strong beam of electrons.

In an attempt to further investigate the properties of the SMOL diffuse “mucus-like” material that held the particulates together, duplicate samples to those that were examined by Bigg et al. (2004) were stored at low relative humidity for 2 to 3 yr before examination. The work was carried out in the Inorganic Chemistry Department of Stockholm University, using a JEOL-2000FX TEM with 200 kV accelerating voltage having an attached X-ray backscatter facility. Blank grids were first used to establish background noise and unwanted signals. Carbon and oxygen signals were present because of the plastic film of the grid, while the grid bars gave a strong copper signal. A background trace from a particle-free area preceded each group of analyses to establish these signals and extract them from the particle analyses. Instead of being unshadowed, as in Bigg et al. (2004), some grids were shadowed with silver for other purposes. This did not mask the signal from the commonly observed elements.

### 3.3. Counting and sizing airborne particulates resembling those of the open leads

The method of sizing the airborne particle that occurred singly or in clusters was similar to that used in the sizing of the open lead surface microlayer particulates described by Bigg et al. (2004). It involved a shape assumption based on the appearance of shadowed specimens. Spheres could approximate most of the particulates, including the angular specimens. Where the individual particles could be distinguished they were sized separately, even though they were in contact with others. Aggregates in which many of the components were hidden were sized as single entities. Viruses would inadvertently have been included since it was not possible to identify them positively from their morphology. The sizes of bacteria in air and in the SMOL were considered separately. For comparison with the number size distributions of the particles photographed by TEM, an aerosol differential mobility particle sizing system (DMPS) that detected particles between about 3 and 900 nm geometric diameter was used. Within the size range of our collections the DMPS records usually showed two modal groups. The first, with its peak in the range 20–40 nm geometric diameter is known as the Aitken mode, while the second at 90–120 nm geometric diameter is called the accumulation mode. Here the terms will be more broadly used to include particles between 15 and 70 nm (Aitken mode) or greater than 70 nm up to the limiting size collected of about 1  $\mu\text{m}$  geometric diameter (accumulation mode).

## 4. Results: comparison of the properties of particulate matter in the atmosphere with those in the surface microlayer of open leads

### 4.1. Morphology and elemental composition of particle aggregates and their building blocks and of bacteria and other micro-organisms

*4.1.1. Particle aggregates and their building blocks.* Atmospheric aggregates were non-hygroscopic and heat resistant and either lay flat on the surface or were in more compact shapes. They came in many sizes, ranging from two to hundreds of components, the components being typically <50 nm DES. The airborne particle of Fig. 2A and the SMOL particle of Fig. 2B had the appearance of small particles strongly welded together. In others the individual components were more distinct as in the airborne Figs 2C and 2D and the SMOL Fig. 2E. Aggregates in the air were often accompanied by widespread diffuse and nearly electron-transparent material (Fig. 2D).

Five X-ray analyses of the atmospheric group showed sulfur and silicon as the major inorganic components but the relatively weak signals suggested a mainly organic composition. According to Bigg et al. (2004) the relatively weak elemental signatures in X-ray analyses of the SMOL samples also suggested a mainly organic composition.

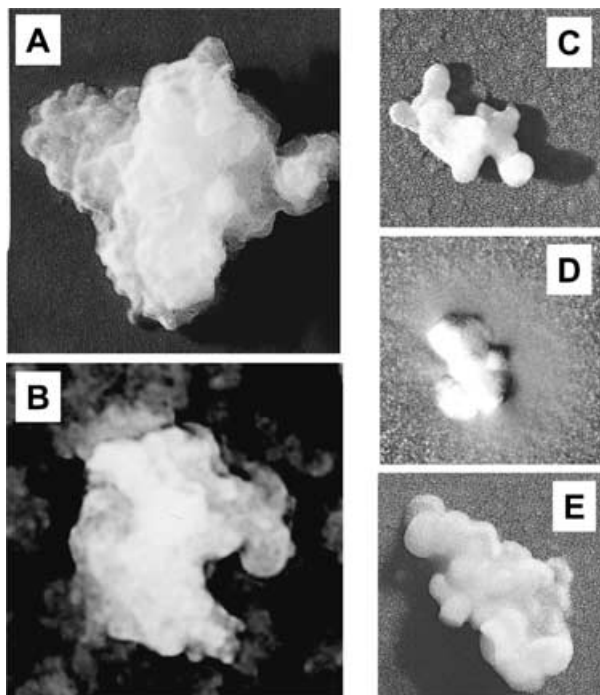


Fig. 2. Some particle aggregates in the air (A, C, D) and in the SMOL (B, E). Diameters of spheres having the same volume (DES): A, 545 nm; B, 95 nm; C, 121 nm; D, 110 nm; E, 186 nm.

Some examples of single airborne particulates that resembled in appearance the building blocks of the aggregates are shown in Figs 3A and 3B. Those in Fig. 3A were surrounded by diffuse material, an angular interior being suggested by the two furthest to the right. The presence of grouped but separated particles was also noted by Bigg and Leck (2001) in a few samples from an earlier expedition to the same general area. Single angular airborne particles, typically collected about 40 nm DES, were more common. Figure 3B is an example of the non-hygroscopic crystalline particles without associated diffuse material, previously noted by Bigg and Leck (2001) frequently to have pentagonal or hexagon habits. An aggregate with smaller components and some associated diffuse material is seen in Fig. 3C. There were many single angular particles in the SMOL samples, but their outlines were usually broken by small attached fragments and larger aggregates. When shadowed with silver, a partial separation of the small and large particles occurred, allowing some of these shapes to be recognized. Figure 3D shows an example.

**4.1.2. Bacteria and other micro-organisms.** The left column of Fig. 4 illustrates some of the micro-organisms, or fragments of them found in the atmosphere, while the right column shows some of those in the SMOL. Figures 4A and 4B show bacteria, those in the water looking much better preserved and having diffuse material attached to them. Figures 4C and 4D include small virus-like particles having angular bodies and tails. Those in Fig. 4C are in a diffuse matrix of partially electron-transparent

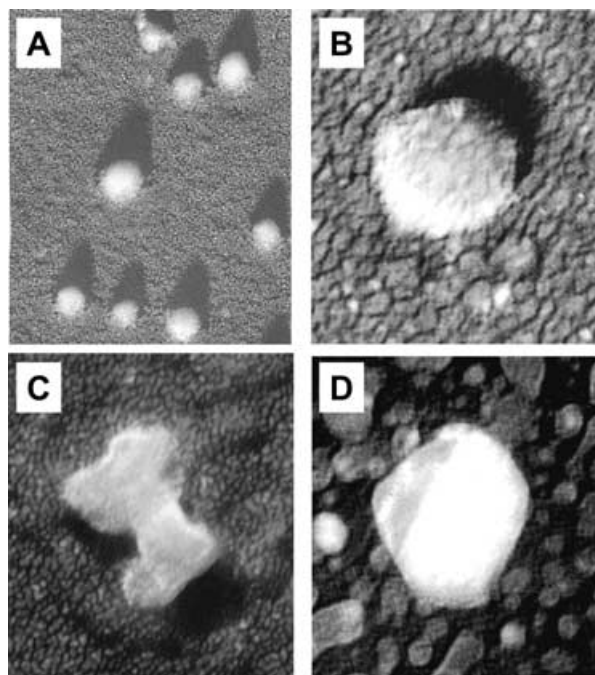


Fig. 3. (A, B) Individual airborne particles, A with and B without visible diffuse material. C shows an aggregate of smaller particles with some diffuse material, while D shows individual particles in the SMOL after separation following silver shadowing. DES: A, 38–57 nm; B, 35 nm; C, 47 nm; D, ~40 nm.

material while those of Fig. 4D are the small particles near a bacterium. Figures 4E and 4F are fragments of diatoms.

#### 4.2. Properties of the diffuse material surrounding particles

Duplicate TEM grids from the SMOL were stored for 2 to 3 yr in a container with dry silica gel and showed some very noticeable differences from grids examined within 3 months of collection. The thin very electron-transparent layer of “mucus-like” diffuse material joining the SMOL particles illustrated by Bigg et al. (2004) had contracted into isolated patches of more electron-dense material that obscured the particles beneath them, as seen in the examples of Fig. 5. X-ray spectra of representative particle groups linked by a thin layer of diffuse material in the early specimens showed few signatures of elements more than two standard deviations above background ( $2\sigma$ ). Chlorine, sodium and silicon were clearly the most abundant, with phosphorus being the other most often detected element. Sulfur, potassium, calcium and magnesium were less frequently detected. Analysis of the more electron-dense patches of diffuse material resulting from ageing of stored specimens had much the same sodium content as the earlier samples, but were greatly richer in three elements. Sulfur predominated, more than  $10\sigma$  in the five determinations, with chlorine and phosphorus being the second most abundant

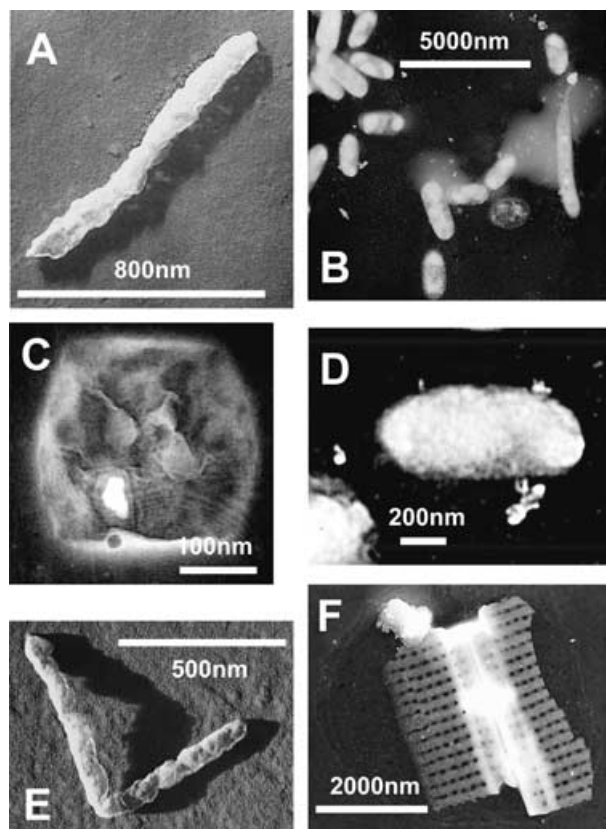


Fig. 4. Micro-organisms or their fragments in air (left column) and in the SMOL (right column): A, B, bacteria; C, D, virus-like particles; E, F, fragments of diatoms.

(about  $5\sigma$ ). Another difference from the SMOL samples was the occurrence of groups of crystalline material not previously seen. These were very rich in chlorine (four determinations), up to  $28\sigma$ , but not in any other element.

A further difference lay in the reaction with silver described by Bigg et al. (2004). In those, the “mucus-like” diffuse material appeared to conduct the silver into the particle groups, which then partially separated into large and small components, as in the example of Fig. 3D. When airborne aggregate particles surrounded by diffuse material were shadowed with silver, the silver was apparently transferred to the particles, making them very opaque to electrons. In the example of Fig. 6A, the black portion represents an area protected from silver during shadowing. It shows that the bulk of the particle disappeared after shadowing, leaving portions of the included aggregate separated on the surface. Aggregates surrounded by diffuse transparent material such as that of Fig. 6B (or Fig. 2D), were electron-dense even when shadowed with a non-reactive metal. However, those that had been stored for long periods appeared to have dried out and had no visible diffuse material around them. The example of Fig. 6C was shadowed with silver, but unlike the particle of Fig. 6B formed a shadow and did not contract, separate into its components or become noticeably more electron-dense. Small holes were visi-

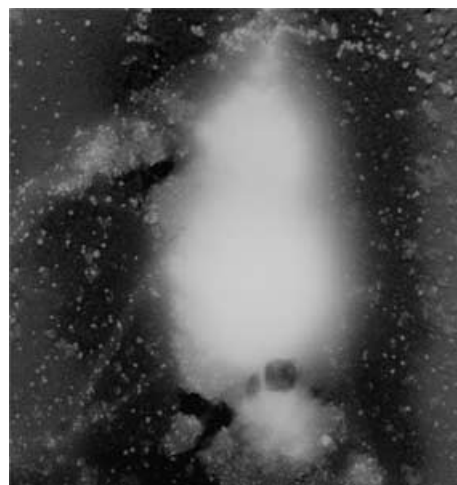


Fig. 5. Retraction of the thin layer of gel into a concentrated patch in a SMOL sample stored for more than 2 yr at low humidity.

ble in many of the individual components, suggesting that they were now partly collapsed hollow shells.

#### 4.3. The proportion of airborne particulate matter thought to originate in the SMOL

The objective method of scanning a TEM grid and photographing every particle encountered allowed an estimate of the ratio of airborne bacteria and other micro-organisms, aggregates and single angular particulates to other collected particles. Table 1 shows that of the 1240 particles photographed on average 56% are likely to have originated in SMOL. Relative to the DMPS total, bacteria and other micro-organisms would represent a smaller proportion than that shown in column B because the total particles counted by the DMPS system usually contained particles which were too small to be efficiently captured by the collectors used. The proportion represented by aggregates and single angular particles might, however, be higher than that in column C since so many of them are  $<15$  nm DES and would not have been collected. Collection efficiency was not a strong influence on the number of internally mixed particles included in column D, but the opacity to electrons of many may have led to an underestimate of their number.

In some cases it was difficult to decide in which category a particle should be placed, and there are unknown errors involved in estimating the proportion of the particulate matter to DMPS-estimated aerosol concentration. Nevertheless it is clear that numerically the particulate matter represents a very substantial part of the total central Arctic Ocean summer aerosol.

#### 4.4. Sizing of the airborne particulate matter

4.4.1. Size distributions of the aggregates and their building blocks. Between 00:00 h on 2 August (DOY 214) and

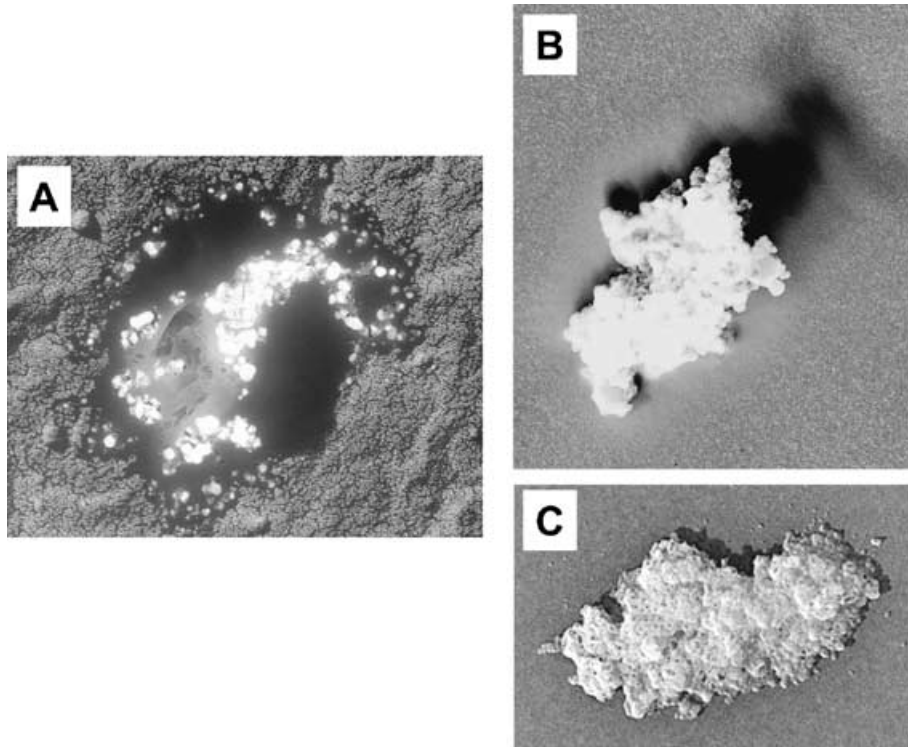


Fig. 6. (A) The effect of shadowing with silver on an airborne particle surrounded by gel. No shadow is formed. The black area (protected from silver), about 1000 nm in diameter, shows the original extent of the particle during shadowing. (B) An airborne aggregate surrounded by a thin layer of diffusing material (DES 555 nm). (C) A similar particle after long storage at low humidity, then shadowing with silver, DES 633 nm.

00:00 h 5 August (DOY 217) 2001, the proportion of collected particles that were aggregates and single angular particles in the TEM collections was more than twice that on other days (*cf.* Table 1). The short time period and the relatively stable and long residence time of the air over the pack ice from air trajectory analysis (175 h) recommended this period for detailed study of size distributions. The method used to form those distributions was described in Section 3.3.

Figure 7a compares TEM size distributions of the particle aggregates shown in Fig. 2. While the shape of the distributions of the air and water aggregates were very similar, with a well-defined mode, the entire airborne distribution is shifted to smaller sizes. Airborne small aggregates appeared identical to parts of large ones, suggesting that one cause of the different size distribution is a progressive breakdown to smaller units in the atmosphere.

The size distribution of single particles shown in Fig. 3B and the component particles of the airborne aggregates is compared in Fig. 7b, illustrating the type of distribution that would result from complete separation of the components of the aggregates.

However, the actual size distribution would have included both unbroken and partially broken aggregates as well as the components. Fig. 7c shows the combined size distribution between DOY 214–216 and compares it with that taken for all TEM collections made over the pack ice. The similarity of the two size

distributions shows that the period of 2–4 August was representative of the whole period spent within the pack ice region.

An independent estimate of size distribution is available from the DMPS records. Confining this to cases within the entire pack ice period, and to residence times of the air over the pack ice exceeding 120 h, Fig. 7d compares the size distribution with the whole-period TEM distribution of Fig. 7c. There are two main differences. Below 15 nm diameter the DMPS records showed many more particles than in the TEM distribution. There are two contributing causes. One is the poor collection efficiency of our TEM samplers below 15 nm DES, the other is that formation of new particles from 3 to 15 nm diameter occurred on a number of occasions. These may have been secondary rather than primary particles. There were also more particles >70 nm diameter in the DMPS curve which we interpreted to be particles having a different nature to the aggregates. There is a remarkable similarity between the size of the Aitken mode in the TEM and DMPS distributions.

*4.4.2. Length and width of bacteria.* Figure 8 compares lengths and widths of airborne bacteria with those in the SMOL. Although their lengths are comparable, the widths of the airborne bacteria are only about one-quarter of those of the SMOL bacteria. Assuming that they are from the same species assembly, those that have been airborne have shrunk very considerably, as implied by their wrinkled appearance. Since both groups have

*Table 1.* Particle types by DOY from TEM photographs. Only days where more than 20 particles were photographed have been included. In total 1240 particles were counted. A: number of particles photographed. B: percentage of total judged to be bacteria and micro-organisms, or fragments of them. C: percentage of single angular particles and aggregates when added to those of column B. D: percentage of total when visible inclusions of type C could be recognized inside other particles (internally mixed)

DOY	A	B (%)	C (%)	D (%)
187	78	15.8	57.9	73.7
190	38	2.6	26.3	36.8
193	31	16.1	29.0	51.6
197	72	1.4	18.1	29.2
203	24	8.3	29.2	37.5
214	28	7.1	57.1	60.7
215	76	6.6	63.2	65.8
216	36	19.4	80.6	80.6
218	43	7.0	34.9	62.8
219	50	2.0	36.0	54.0
220	51	33.3	80.4	100.0
221	25	0.0	12.0	52.0
222	120	0.0	15.8	25.0
223	62	6.5	16.1	38.7
225	30	0.0	46.7	53.3
226	52	5.8	30.8	67.3
227	80	1.3	37.5	87.5
228	29	3.4	3.4	24.1
229	45	0.0	22.2	33.3
230	81	3.7	24.7	30.9
231	105	21.9	55.2	80.0
233	56	7.1	51.8	73.2

been subjected to the vacuum of the electron microscope, those in the air must have lacked some protection from dehydration possessed by those from the SMOL samples.

Moreover, there is a subclass of rod-shaped objects with rounded ends in both the air and the SMOL. While these look like bacteria, their median length of 200 nm and width of about 50 nm (not greatly different between air and water particles) suggests that they are either fragments of other organisms or rod-shaped viruses.

### 5. Discussion

#### 5.1. The “mucus-like” diffuse material accompanying particulates

The possible atmospheric importance of the “mucus-like” diffuse material accompanying particles in the SMOL was emphasized in the Introduction. Our results have shown that it is also commonly present around atmospheric particles, has a strong affinity for silver, has a limited lifetime in the atmosphere or if stored for long periods at low humidity, but can survive rapid evacuation in

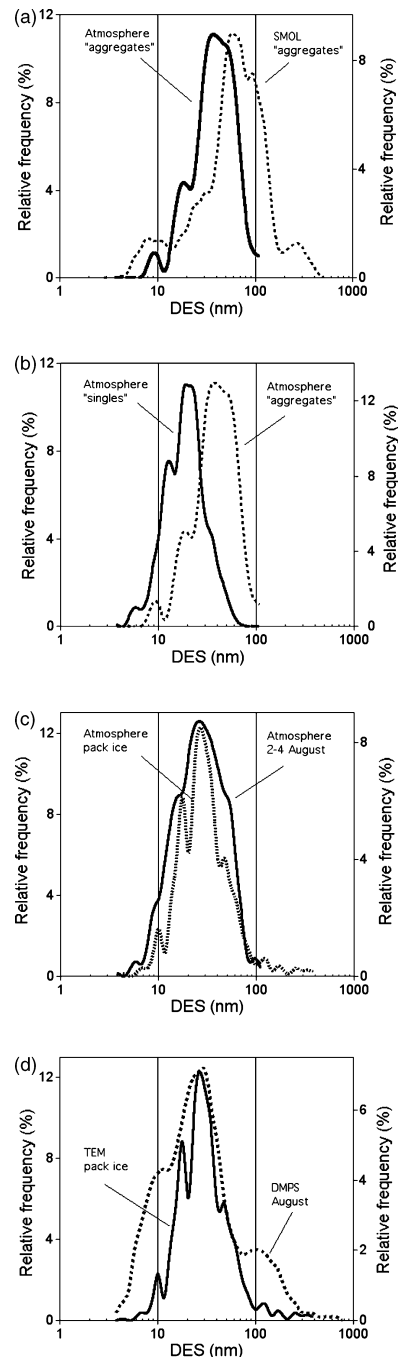


*Fig. 7.* Comparison of size distributions of particulates in air and SMOL. (a) Comparison of TEM airborne and SMOL aggregate size distributions. (b) Comparison of the TEM size distribution of single particles and components of airborne aggregates with that of the aggregates. (c) Combined TEM size distribution of single particles, aggregates and their components for the period of intense study, 2–4 August, with that of the entire period spent within the pack ice. (d) Comparison of the overall airborne size distribution from the DMPS system (periods with residence times of the air over the pack ice > 120 h only) with TEM combined size distribution (c) for the entire period spent within the pack ice.

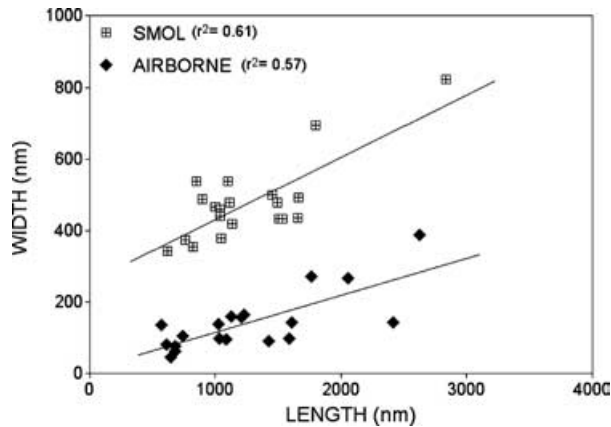


Fig. 8. The relationship between length and width of airborne and SMOL bacteria.

an electron microscope. Microalgae and bacteria in sea water are known to produce copious amounts of large molecules having a “mucus- or gel-like” consistency usually referred to as exopolymer secretions (EPS). A comprehensive review of the EPS of microalgae and bacteria has been given by Decho (1990). The information detailing properties that might be relevant to our observations is summarized below.

The purpose of EPS is to concentrate nutrients around the organism and to protect it from toxins. Exopolymers are very surface active, highly hydrated molecules, mainly polysaccharides of molecular weight 100–300 kDa and may contain 99% water. Microalgal EPS has a pH-dependent binding of metal ions that is most effective at the pH of sea water and has been observed to remove 99% of silver ions. EPS has a strong affinity for chlorine, reducing the effectiveness of chlorine bactericides. Krembs et al. (2002) have shown that sea-ice microalgae are prolific producers of EPS that can act as a cryoprotectant and regulator of osmotic changes. EPS contain polysaccharide chains bridged with divalent ions such as  $\text{Ca}^{2+}$  and  $\text{Mg}^{2+}$ , to which can be attached both high-molecular-weight molecules such as proteins and peptides and smaller groups such as amino acids, sulfates and phosphates.

Chin et al. (1998) noted that a lowering of pH to 4.5 causes a sudden transition of EPS gels in which the polymer network collapses to a dense non-porous array. While this would not happen in sea water where the pH is 8, if an EPS gel was transferred to the atmosphere and divorced from accompanying sea water it might be of importance. Furthermore, Orellana and Verdugo (2003) investigated the effects of ultraviolet (UV) light on EPS gels, showing that it splits the polysaccharides into smaller units that cannot reassemble.

The properties of EPS listed above are just those that would explain those of the diffuse material that we have observed around particles in the SMOL and in the air. In the SMOL samples it was seen around bacteria (Fig. 4B) and the highly trapped water content of the EPS would allow it to protect the bacteria during

exposure to a vacuum. The chlorine, sulfur and phosphorus that we observed in the stored SMOL specimens are consistent with the affinity of EPS for those elements, and the reaction with silver would be expected because of its very strong binding to that element. Furthermore the observed morphological changes such as the difference between the airborne particles of Figs 6B and 6C and the shrinking of airborne bacteria and aggregates would be expected on the basis of the properties of EPS gels. As a result of the loss of water on collapse, reactivity to silver would be reduced, as we have observed.

We will therefore refer in future to the “mucus-like” diffuse material observed in this study as an “EPS gel”. According to Chin et al. (1998) only 10% of marine polymers take part in the formation of microgels. The proportion of the remaining 90% that should be considered part of the EPS has not been stated. For simplicity we use the term above except where unassembled surfactant polymers may be important. Then “EPS” alone will be used.

It may be thought that transport of EPS to the atmosphere would alter the conclusions as to its fate in the ocean. However, even if all the airborne particles consisted of EPS, its mass there would be completely insignificant compared with that in the surface mixed layer of the ocean.

### 5.2. The apparent absence of sea salt on marine bacteria and aggregates

One of the features of single-particle analysis in a marine environment is the apparent absence of sea salt on particles such as bacteria that have obviously come from the sea. It was noted by Gras and Ayers (1983), Leck et al. (2002), Pósfai et al. (2003) and in the present work, and has been difficult to explain. A separation during crystallization of the sodium chloride is a possible hypothesis in a humidity below the deliquescence point of 75% (Tang and Munkelwitz, 1993) but cannot be used in the Arctic where the near-surface relative humidity was close to 95% most of the time. In the next section, the possibility will be explored that the initial presence of EPS on particles transferred from sea to air might be responsible.

The great affinity of EPS for water ensures that it will play a large part in determining the properties of bubbles produced in sea water and the fragments produced when the bubbles burst. Zhou et al. (1998) have examined the foam produced by bubbling sea water, finding that it contained highly surface-active polysaccharides. Sulfur was present in the form of sulfate half-esters. During AOE-2001 Knulst et al. (2003) found that the surface tension of the SMOL of the open leads was lowered, showing the presence of such surfactants.

Blanchard (1958) pioneered the study of the production of airborne particles by bursting bubbles. He showed that there are two distinct processes—the production of fragments from the bubble wall (“film drops”) and drops of sea water ejected from the surface at the centre of the bubble following bursting (“jet drops”).



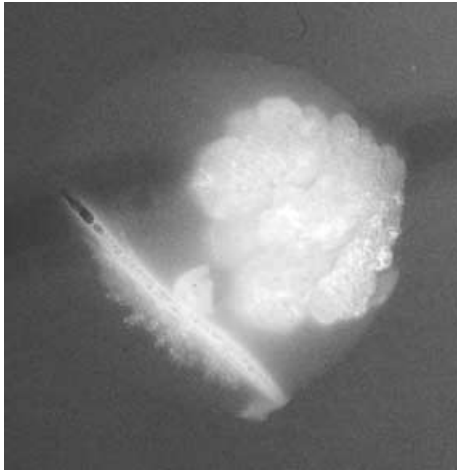


Fig. 9. A particle aggregate in the atmosphere surrounded by gel. It also contains a bacterium attached to a small aggregate possibly detached from the larger one. The DES of the larger aggregate is about 630 nm assuming that the thickness is equal to the width of the largest component.

Blanchard (1964) also recognized the role of the organic film on the sea surface in injecting organic material into the atmosphere when bubbles burst. Since that time, however, it has usually been tacitly assumed that bubble walls consist of sea water with perhaps a small admixture of surfactants. If instead bubble walls are composed mainly of EPS surfactants, they would be more resistant to breaking than ones composed only of sea water. In the absence of external forcing such as strong winds, bubbles would only break after excess water had drained off and the bubble film thinned sufficiently by gravitational forces. Figure 9 shows an aggregate surrounded by transparent material that we assume to be an EPS gel. It also includes a bacterium attached to a smaller aggregate possibly detached from the larger one. We believe the Figure 9 particle to be an examples of a “film drip”—fragments of the bubble wall that contained particulates. If the EPS gel around the aggregate shown in this figure collapses once airborne due to UV or lowering of pH to 4.5 or less, the trapped water would be expelled, leaving the particles free from salt.

What would happen to the expelled water? If it is a sodium chloride solution, a drop or drops of solution would appear in the atmosphere and be seen in the electron microscope as very small crystals since the salt content is at most 3%. We are dealing here with low-wind situations where sea salt crystals <200 nm diameter were not in evidence either in the particle collections or in size-segregated chemical analysis. One possibility is that since one of the functions of EPS is to regulate osmosis, the salt content of the trapped water may be low. The X-ray analyses of SMOL samples showed relatively weak sodium signals and a large excess of chlorine compared with sea-salt ratios. This also suggests that the trapped water of the EPS gel was much less salty than sea water.

Except in strong wind conditions sea-salt particles produced by the jet drops that follow bubble bursting were not sufficiently numerous relative other particles to occur in our collections. Bacteria or aggregates carried up with these drops will have less EPS gel around them and will be likely to retain sea salt on them.

### 5.3. Physical and chemical transformations of airborne particulates originating in the SMOL

The marked differences in length-to-width ratios of airborne and SMOL bacteria seen in Fig. 8, and the wrinkled appearance of the former but not the latter, are examples of physical changes that occur when particles from the SMOL become airborne.

However, the airborne bacteria from the Southern Ocean illustrated by Pósfai et al. (2003) look as well preserved as our SMOL bacteria. The time for which particles are exposed in the atmosphere will obviously be important for the extent of physical or chemical change, and this may explain the difference. The flux of particles from open leads in the pack ice was shown by Nilsson et al. (2001) to be an order of magnitude smaller than that from the open ocean, and open leads occupied only 5–20% of the area. Although the flux is therefore small, it will operate over a very large area so that most particles will have had atmospheric residence times of hours or even days. In contrast, the most likely source of the Southern Ocean bacteria of Pósfai et al. (2003) is the extensive beds of macroalgae immediately upwind from the collection point at Cape Grim, giving them an atmospheric residence time of minutes.

Chemical as well as physical transformations of atmospheric particulates will occur if UV light or acidification shortens the polysaccharide chains of associated EPS gels. This will lead to the release of high-molecular-weight organic compounds attached to the chains, which may in turn be broken into smaller units. Some of these may be soluble in organic vapours such as decane, unlike the polysaccharide assemblies. Confirmation of this can be seen in the spectacular effect of decane vapour on an aged film drop particle shown by Leck et al. (2002) (their Fig. 6c).

Figure 10 gives another example, an aggregate particle that probably originally looked like that of Fig. 9b after being exposed to decane vapour. Material surrounding the aggregate has dissolved and spread out on the surface as a thin layer, while one of its components formed the white crystals when the decane evaporated. The gels in the microlayer, or those similar to the particle of Fig. 9b, are unaffected by decane, suggesting that in this particle a chemical transformation to lower-molecular-weight compounds has occurred.

The chemical transformation of the EPS gel could also lead to a weakening of the bonds joining aggregates and allow their fragmentation. The difference in airborne and SMOL size distributions shown in Fig. 7a is consistent with this cause. A result of fragmentation would be to generate an externally mixed Aitken mode consisting of hydrophobic particles that have lost all their

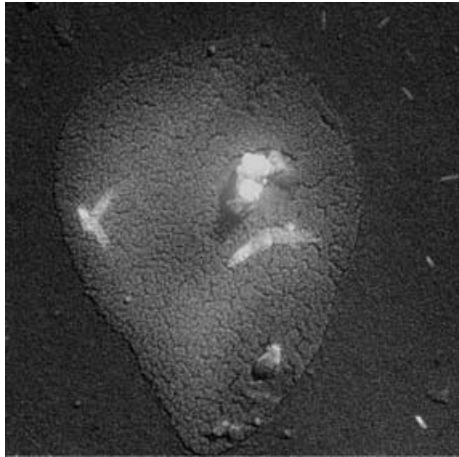


Fig. 10. A particle aggregate (DES 125 nm) after being subjected to decane vapour that has dissolved the surrounding organic material and spread it into a thin layer.

surface-active covering and hydrophilic particles where that covering remains.

#### 5.4. Origin of the Aitken mode particles in the Arctic

The origin of the numerous Aitken mode particles over the pack ice having a crystalline appearance, discovered by Leck and Bigg (1999), was difficult to reconcile at the time of their first collection.

Although the DMPS records showed many occasions with relatively high concentrations of particles <50 nm diameter, the only types encountered in our collections during either AOE-96 or AOE-2001 resembled the airborne particles of Figs 2 and 3. The possibility that aggregates (Fig. 2) containing hundreds of <50 nm diameter particles might separate into large numbers of single particulates mostly too small to be captured by our collectors seems to provide a solution. The remarkable agreement between the modal size of DMPS and TEM distributions of Fig. 2D gives support to this suggestion.

#### 5.5. Influences of the SMOL particles and EPS on concentrations of cloud condensation nuclei (CCN)

In an attempt to simulate observed CCN concentrations for air that had spent several days over the pack ice, Lohmann and Leck (2005) found it necessary to invoke a highly surface active Aitken mode externally mixed with a sulfur-containing population. Particles such as those of Figs 3A and 3C having visible amounts of what is assumed to be EPS with highly surface-active properties, give extra weight to that suggestion. Cloud activation of particles of the type seen in Figs 3A and 3C will, through aqueous oxidation of sulfur dioxide, lead to the formation of an internally mixed predominantly sulfur-containing aerosol particles.

The transient nature of the EPS in the atmosphere due to degradation by UV or acidification means that particles originating in

the SMOL will eventually lose their surfactant content, leading to a mixed population of surface water-active and water-inactive Aitken mode particles. Those that are water-inactive are likely to act as sites for acquisition of the oxidation products of DMS, leading to the formation of sulfur-containing CCN. If this supposition is correct, sulfur-containing particles should contain aggregates or their components from the SMOL, and this possibility will be explored in a subsequent paper.

If the radiative properties of the boundary layer clouds have an influence on climate, and if particles from the SMOL are both CCN in their own right or centres for the acquisition of sulfate, then there will be more complex potential aerosol–climate feedback processes between the microbiology of the region than from DMS alone (Charlson et al., 1987). The oxidation products of DMS will determine the ultimate size to which the particles will grow, but the primary nuclei will determine how many of them there will be. It is the number of activated CCN that determines the albedo of a cloud and its effect on radiation.

#### 5.6. Schematic representation of the processes described in this study

The schematic diagram of Fig. 11 may help in understanding the processes described in the discussion. The water part of Fig. 11 shows typical aggregates joined with EPS and a bacterium surrounded by EPS gel. If a bubble is present in the water from any cause, it will scavenge aggregates of small particulates, bacteria and EPS gels from the water in its rise to the surface. When the bubble bursts, it will lead to film drops (left branch) containing EPS gels micro-organisms and aggregates. Jet drops are also produced (right branch) containing sea salt, EPS and any larger particles not scavenged by the bubble walls. The aggregates of the left branch progressively split apart as the gel collapses due to the influence of UV light and acidification, ultimately forming the Aitken mode seen by the DMPS in Fig. 7d.

## 6. Conclusion

This work has shown that particulate matter from the surface microlayer of the open leads of the central Arctic Ocean, including micro-organisms, small water-insoluble particles and aggregates of them, can form a substantial part of the summer aerosol in that region. It has demonstrated that the “mucus-like diffuse”, almost electron-transparent material binding the particles of the SMOL (Bigg et al., 2004) can be identified with the exopolymer secretions of bacteria and microalgae.

Identification of EPS on airborne particles leads to further conclusions. One is that it must modify the bubble-bursting process that allows sea-to-air transfer of particulates. Another is that the associated surfactants will confer cloud-nucleating properties on the water-insoluble particles from the SMOL until UV or other influences destroy their surface activity. A mixture of young and aged atmospheric particles derived from the SMOL

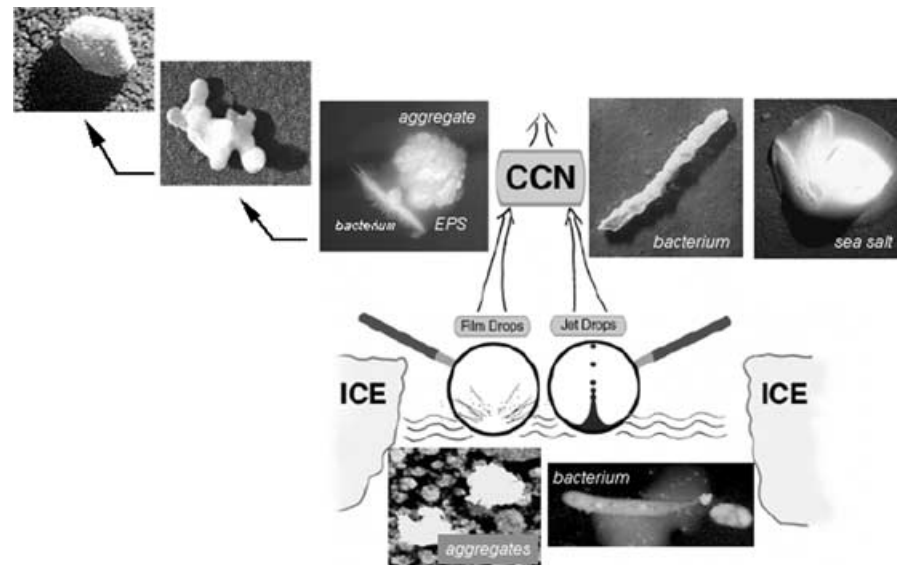


Fig. 11. A schematic representation of the particle production and dispersal processes described in this paper.

will then create an externally mixed Aitken mode consisting of water-active and water-inactive particles.

EPS occur in all the world's oceans, with the highest concentrations in biologically productive regions. It is therefore likely that similar processes to those we have described will play some part in the production and evolution of the marine aerosol everywhere. In that case potential climate–aerosol feedback processes may differ considerably from those suggested by Charlson et al. (1987). Attention should therefore be directed towards studying the detailed nature of individual marine airborne particles. While electron microscopy is time-consuming, it is at present the only way that an insight into the history of particles smaller than 100 nm diameter can be obtained.

## 7. Acknowledgments

Agneta Öhrström's invaluable help in the tedious analysis of size distributions of surface microlayer particles and in obtaining large numbers of X-ray spectra is greatly appreciated. Special thanks goes to Birgit Wehner for providing the DMPS data. We thank Dr Ian Kaplin of Sydney University's Electron Microscope Unit for his assistance with the TEM photographs reproduced here. We should also like to thank the Swedish Polar Research Secretariat and the Captain and crew of the icebreaker *Oden* for their logistical support. The financial support from the Swedish Natural Science Research Council (CL), the International Meteorological Institute and the Knut and Alice Wallenberg Foundation is gratefully acknowledged (CL).

## References

- Bigg, E. K. and Leck, C. 2001. Properties of the aerosol over the central Arctic Ocean. *J. Geophys. Res.* **106**(D23), 32 101–32 109.

- Bigg, E. K., Leck, C. and Tranvik, L. 2004. Particulates of the surface microlayer of open water in the central Arctic Ocean in summer. *Marine Chem.* **91**, 131–141.
- Blanchard, D. C. 1958. Electrically charged drops from bubbles in sea water and their meteorological significance. *J. Meteorol.* **15**, 383–396.
- Blanchard, D. C. 1964. Sea-to-air transport of surface active material. *Science* **146**, 396–397.
- Charlson, R. J., Lovelock, J. E., Andreae, M. O. and Warren, S. G. 1987. Oceanic phytoplankton, atmospheric sulphur, cloud albedo and climate. *Nature* **326**, 655–661.
- Chin, W.-C., Orellana, M. V. and Verdugo, P. 1998. Spontaneous assembly of marine dissolved organic matter into polymer gels. *Nature* **391**, 568–572.
- Decho, A. W. 1990. Microbial exopolymer secretions in ocean environments: their role(s) in food webs and marine processes. *Oceanogr. Mar. Biol. Ann. Rev.* **28**, 73–153.
- Gras, J. L. and Ayers, G. P. 1983. Marine aerosol at southern mid-latitudes. *J. Geophys. Res.* **88**, 10 661–10 666.
- Knulst, J. C., Rosenberger, D., Thompson, B. and Paatero, J. 2003. Intensive sea-surface microlayer investigations of open leads in the pack ice during Arctic Ocean 2001 expedition. *Langmuir* **19**(24), 10 194–10 199.
- Krembs, C., Eicken, H., Junge, K. and Deming, J. W. 2002. High concentrations of exopolymeric substances in Arctic winter sea ice: implications for the polar ocean carbon cycle and cryoprotection of diatoms. *Deep Sea Res.* **49**, 2163–2181.
- Leck, C. and Bigg, E. K. 1999. Aerosol production over remote marine areas—a new route. *Geophys. Res. Lett.* **23**, 3577–3581.
- Leck, C., Larsson, U., Bågander, L. E., Johansson, S. and Hajdu, S. 1990. DMS in the Baltic Sea—annual variability in relation to biological activity. *J. Geophys. Res.* **95**, 3353–3363.
- Leck, C., Nilsson, E. D., Bigg, E. K. and Bäcklin, L. 2001. The atmospheric program on the Arctic Ocean Expedition in the summer of 1996 (AOE-96)—a technical overview. Outline of experimental

- approach, instruments, scientific objectives. *J. Geophys. Res.* **106**(D23), 32 051–32 067.
- Leck, C., Norman, M., Bigg, E. K. and Hillamo, R. 2002. Chemical composition and sources of the high Arctic aerosol relevant for fog and cloud formation. *J. Geophys. Res.* **10**, doi:10.1029/2001JD001463.
- Leck, C. and Persson, C. 1996. The central Arctic Ocean as a source of dimethyl sulfide—seasonal variability in relation to biological activity. *Tellus* **48B**, 156–177.
- Leck, C., Tjernström, M., Matrai, P., Swietlicki, E. and Bigg, E. K. 2004. Can marine micro-organisms influence melting of the Arctic pack ice? *EOS Trans.* **85**(3), 25–36.
- Lohmann, U. and Leck, C. 2005. Importance of surface-active organic aerosols for pristine Arctic clouds. *Tellus* **57B**, 261–268.
- Nilsson, E. D., Rannik, Ü., Swietlicki, E., Leck, C., Aalto, P. P. and co-authors 2001. Turbulent aerosol number fluxes during the Arctic Ocean Expedition 1996, part II: a wind driven source of sub micrometer aerosol particles from the sea. *J. Geophys. Res.* **106**(D23), 32 139–32 154.
- Orellana, M. V. and Verdugo, P. 2003. Ultraviolet radiation blocks the organic carbon exchange between the dissolved phase and the gel phase in the ocean. *Limnol. Oceanogr.* **48**, 1618–1623.
- Pósfai, M., Li, J., Anderson, J. R. and Buseck, P. R. 2003. Aerosol bacteria over the Southern Ocean during ACE-1. *Atmos. Res.* **66**, 231–240.
- Tang, I. N. and Munkelwitz, H. R. 1993. Composition and temperature dependence of the deliquescence properties of hygroscopic aerosols. *Atmos. Environ.* **27A**, 467–473.
- Wells, M. L. and Goldberg, E. D. 1991. Occurrence of small colloids in seawater. *Nature*, **353**, 342–344.
- Zhou, J., Mopper K. and Passow, U. 1998. The role of surface-active carbohydrates in the formation of transparent exopolymer particles (TEP) by bubble absorption of seawater. *Limnol. Oceanogr.* **43**, 1860–1871.